

Thermal analysis of PVA/CNTs 2D membrane

Sangram K. Samal · Elizabeth G. Fernandes ·
Federica Chiellini · Emo Chiellini

AICAT2008 Conference
© Akadémiai Kiadó, Budapest, Hungary 2009

Abstract In the present study polymeric membranes consisting of poly(vinyl alcohol) (PVA) and multi-walled carbon nanotubes (MWCNTs) were prepared by casting method and their morphological, thermal and de-swelling behaviour were characterized. The effect of MWCNTs in the hybrid membranes was more significant when its concentration was high. The thermo degradation (T_d) and crystallization (T_c) temperatures of PVA increased of 10 and 9 °C, respectively in presence of $50 \times 10^{-2} \text{ w v}^{-1}\%$ of MWCNTs (PVNT3). Besides, the amount of non-free water increases with increasing of MWCNTs probably due to a capillary effect.

Keywords Carbon nanotube · Hydrogel · Nanocomposite · State of water · Swelling · Thermal analysis

Introduction

Carbon nanotubes (CNTs) are attracting interest for their inherent structural features that appear to be prone to open new interesting avenues for novel application in science and technology. The accessible hollow structure may facilitate the flow and migration of metabolites or bioactive agents, and hence may also be used as convenient drug carriers at nanoscale level [1]. CNTs can be ideal candidates to modify the performance of polymeric membranes.

Promising possibilities can be expected on reinforcing of polymeric materials and on providing some specific requested functionality to tissue engineered membranes. Incorporating CNTs into polymeric scaffolds other than improvement in thermal, mechanical and electrical conductivity should be effective in influencing cell growth and providing useful responses for pharmaceutical and tissue engineering regeneration. But the incorporation of CNT into different polymeric matrices are always problematic, it is due to poor solubility and low dispersibility of CNT in water or organic solvents [2, 3].

The water-soluble polyhydroxy polymer as PVA is known as one of the most utilized synthetic polymers, which received increasing attention in biomedical and pharmaceutical applications. Due to PVA biocompatibility and biodegradability it has been used in several biomedical applications such as hydrogels for tissue engineering related to artificial articular cartilage, artificial pancreas and bone-like apatite formation [4, 5]. The specific structure and properties of PVA increases its possibilities to tailoring properties of items obtained by blending it with other compatible polymers of synthetic and natural origin. PVA is also known to provide good stress transfer to CNT when used as continuous matrix in CNT loaded constructs [6].

Membranes have been accepted as an interesting way to provide controlled delivery of drugs and biomolecules to the systemic circulation [7]. The preparation of dense 2D membrane is a viable approach prior to the fabrication of porous 3D scaffolds. The dense 2D membrane scaffolds are crosslinked hydrophilic polymeric chain networks that swell in water or biological fluids. They turned out to be appealing biomaterials for biomedical and pharmaceutical applications including among the other practices drug delivery to a specific target site, tissue engineering

S. K. Samal · E. G. Fernandes · F. Chiellini · E. Chiellini (✉)
Laboratory of Bioactive Polymeric Materials for Biomedical and Environmental Applications, UdR-INSTM, Department of Chemistry and Industrial Chemistry, University of Pisa, Via Vecchia Livornese, 1291 Pisa, Italy
e-mail: emochie@dcc.unipi.it

applications in 2D tissues such as transdermal or articular cartilage, bioseparation and protein folding.

In the present study, the incorporation of MWCNTs into PVA for the preparation of polymeric membrane was investigated. PVA-MWCNTs nanocomposite membranes were characterized morphologically using scanning electron microscopy (SEM), swelling behaviour and thermal stability using thermogravimetric analysis (TGA) and thermal properties and state of water using differential scanning calorimetry (DSC).

Experimental

Materials

Poly(vinyl alcohol) (PVA) with molecular weight (MW) 146–186 kDa and 99% of hydrolysis was purchased from Sigma-Aldrich. Aqueous dispersion of MWCNTs (AQ0101 grade—1 wt% of CNTs) was kindly provided by Nanocyl Company, Belgium. The relevant data sheet does not inform whether MWCNT surface was functionalized but that the dispersion is stabilized with ionic surfactant.

Preparation of membranes

Aqueous PVA solutions and PVA-MWCNTs dispersion were obtained using our previously published protocols [8] with slight modifications and membranes were prepared by solution casting method at room temperature. Briefly, the clear viscous solution of PVA and black colour viscous dispersion of PVA-MWCNTs were obtained by heating them at water boiling point under reflux. After that, the solutions were allowed to cool down to room temperature and then were cast onto a smooth and clean polystyrene Petri dish. Water from cast liquid film was evaporated at room temperature for 48 h. Subsequently, the resultant membranes were oven dried for other 48 h at 37 °C in order to ensure complete removal of remaining water. The resultant membranes were flexible and tough. The PVA based membranes were stored in parafilm closed FalconTM tubes at −4 °C to prevent possible degradation before

submitting them to testing evaluations. Solutions compositions and membrane identification codes are presented in Table 1.

Characterization

The morphologies of membranes to access MWCNTs compatibility and homogeneity were accomplished with a JEOL (JSM-5600LV) scanning electron microscope (SEM) at the required magnification and with accelerating voltage of 14 kV. The film samples frozen in liquid nitrogen were fractured and sputtered with gold before SEM observation.

TGA is commonly used to measure polymer absorbed moisture content, residual solvent levels, degradation temperatures and the amount of non-combustible (inorganic) filler in polymer or composite materials compositions. In this work, TGA experiments were carried out in a TA Instrument model Series Q500 with the Universal TA analysis software. The TGA temperature was calibrated with three standards and the weight with 100 and 1,000 mg standards. The effect of the MWCNTs amount on the pyrolysis behaviour of PVA was evaluated using TGA traces obtained from specimens of 10–15 mg at 10 °C min^{−1} in the range 25–900 °C, under nitrogen flow rate of 60 mL min^{−1}.

The swelling behaviours of PVA based membranes were evaluated by immersing the pre-weighed dried membrane specimens in distilled water at pH 7.4 and 37 °C for 5 days in aqueous medium to obtain the fully equilibrium swollen state. After this time, specimens were withdrawn from aqueous medium and the excess of surface water was removed gently with a wiping paper. Immediately after, their weight was recorded by using an analytical balance and the specimens again returned to the aqueous medium. The swelling degrees (SWD) of membranes were calculated by using the following equation:

$$\text{SWD (\%)} = \left[\frac{(W_s - W_d)}{W_s} \right] \times 100 \quad (1)$$

where W_d and W_s are the weights of dried and swollen hydrogel membrane, respectively.

On the other hand, the de-swelling kinetic was assessed using TGA in isothermal scan mode at 37 °C. The samples were prepared in the same way above described for SWD evaluation. The weight loss from specimens weighing 10–15 mg under a nitrogen atmosphere at a flow rate of 60 mL min^{−1} was followed by a time of 3 h.

DSC evaluations of both state of water inside membranes and thermal parameters of PVA based materials were carried out on a Mettler DSC 822^e module controlled by the STAR^e software under nitrogen atmosphere at 80 mL min^{−1} of flow rate. The weight of samples used on the state of water and thermal parameters evaluations were

Table 1 Solution compositions and codes of PVA/MWCNTs nanocomposites

Sample	PVA/w v ^{−1} %	MWCNTs/w v ^{−1} % 10 ^{−2}
PVA	10	0
PVNT1	10	0.25
PVNT2	10	2.50
PVNT3	10	50.00

w v^{−1}% is the amount in g of material in 100 mL of water

1–3 and 3–9 mg, respectively as weighed in 40 μL aluminium hermetic pan. An empty pan was used as reference. DSC temperature calibration was performed using indium and zinc standards. Measurements for the state of water were performed according to the following protocol:

1. Cooling scan from 25 to -70 $^{\circ}\text{C}$ at 10 $^{\circ}\text{C min}^{-1}$ and isotherm of 5 min at the end temperature and
2. Heating scan from -70 to 50 $^{\circ}\text{C}$ at 10 $^{\circ}\text{C min}^{-1}$.

Thermal properties of the membranes were determined by performing three DSC scans. In particular, the first heating scan was used to erase any prior thermal history of the sample, the intermediate cooling scan established a well defined thermal history and the second heating scan was used to evaluate melting (T_m) and glass transition (T_g) temperatures. Measurements were performed according to the following protocol:

1. First heating scan from 25 to 230 $^{\circ}\text{C}$ at 10 $^{\circ}\text{C min}^{-1}$ and 3 min of isotherm at the end;
2. First cooling scan from 230 to 25 $^{\circ}\text{C}$ at -10 $^{\circ}\text{C min}^{-1}$ and 3 min of isotherm at the end; and
3. Second heating scan from 25 to 230 $^{\circ}\text{C}$ at 10 $^{\circ}\text{C min}^{-1}$.

Results and discussion

The PVA-MWCNTs membranes were transparent and homogeneous with a colour dependent upon the loading of nanotubes. The surface morphologies of PVA-MWCNTs nanocomposite membranes PVNT2 and PVNT3 are shown in Fig. 1a and b, respectively.

Both samples present a spherical motif at $25,000\times$ of magnification, whose size was comprised in a $200\text{--}300$ nm range. They are probably due to some agglomerates of

MWCNTs. This hypothesis can be confirmed comparing the photomicrographs of MWCNTs (Fig. 1c) with that of PVNT3 after pyrolysis (Fig. 1d) where it is possible to observe similar coil arrangement of MWCNTs but with some agglomerates.

Figure 2a shows first derivative TGA (DTG) traces of PVA-MWCNTs nanocomposite membranes compared with pristine components. MWCNTs traces were obtained from cast film of the original aqueous dispersion. All membrane samples presented at least three principal weight loss steps and the first one corresponds to the adsorbed moisture from ambient. This moisture between 7 and 16 wt% (Table 2) remained in all PVA based membranes and pristine components in equilibrium with that of ambient. The second step of MWCNTs corresponds to three overlapped DTG peaks. The maximum degradation rate defined at the peak of the DTG (T_p) was more intense at 363 $^{\circ}\text{C}$, and likely corresponds to the thermal degradation of the surfactant present in their aqueous dispersion.

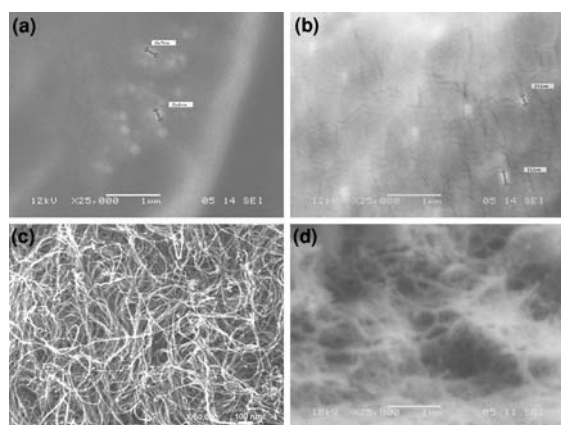


Fig. 1 SEM photomicrographs of PVNT2 (a), PVNT3 (b), MWCNTs (c), and PVNT3 after pyrolysis (d)

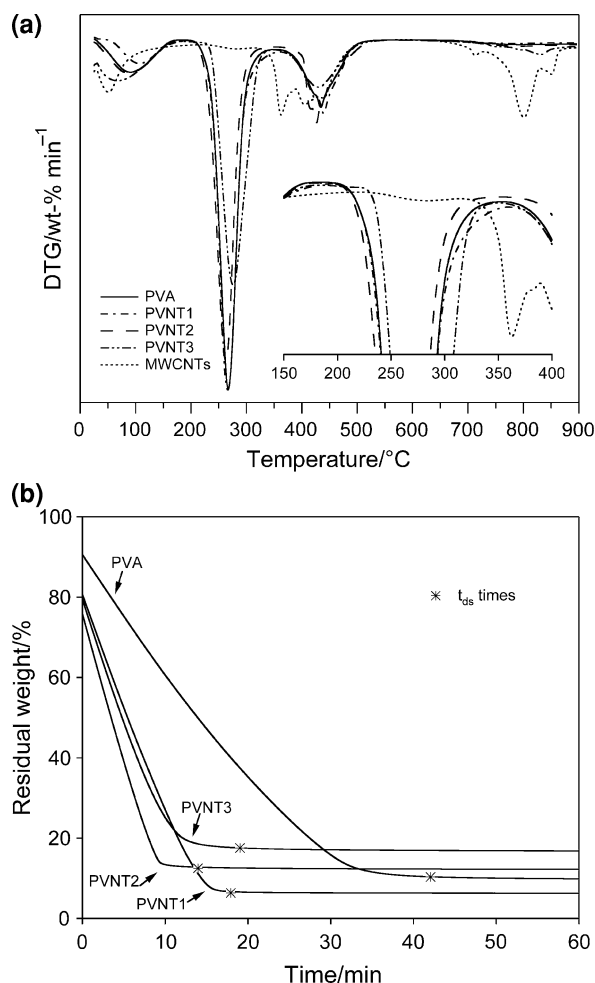


Fig. 2 DTG (a) and de-swelling TGA (b) traces of PVA/MWCNTs membranes

Table 2 TGA data and SWD values of PVA/MWCNTs membranes and pristine components

Sample	Thermal degradation parameters					Swelling/de-swelling		
	Water/%	$T_d/^\circ\text{C}$	$T_{p1}/^\circ\text{C}$	$T_{p2}/^\circ\text{C}$	$T_{p3}/^\circ\text{C}$	$R/\% \text{ min}^{-1}$	t_{ds}/min	SWD/%
PVA	11	234	267	434	–	–3.0	42	270
PVNT1	7	233	267	439	–	–5.5	17	308
PVNT2	12	230	263	426	795	–7.1	15	275
PVNT3	16	244	276	431	832	–5.8	19	174
MWCNTs	15	352	–	$406/363/439$	$713/801/850$			

T_d is the decomposition temperature defined at 2 wt% weight loss and T_p is the maximum degradation rate defined at the peak of the DTG; R is the rate of de-swelling; t_{ds} is the de-swelling time; and SWD is the swelling degree

The third step of MWCNTs has also three overlapped DTG peaks and the T_p value of the principal one is at 801 °C. It is probable that this higher temperature weight loss is due to the gasification of carbon of defected nanotube structures [9]. PVA decomposes in two steps, whose T_p values are respectively 267 and 434 °C. T_p values of PVNT1 and PVNT2 basically did not presented significant changes in relation to that of the pristine PVA. However, the maximum degradation rate of the first step (T_{p1}) on PVNT3 sample increased of 9 °C.

Decomposition temperature defined at 2 wt% weight loss (T_d) [10] of PVA and MWCNTs were 234 and 354 °C, respectively. PVA-MWCNTs membranes decomposed at temperatures between those of the pristine components and the most significant change (10 °C higher than that of PVA) was observed on sample containing $50 \times 10^{-2} \text{ w v}^{-1}\%$ of MWCNTs (PVNT3) as can be noted in the zoom inside DTG picture (Fig. 2a). This result substantiates the characteristic of the nanoparticles to improve thermal stability of polymeric composites [11].

De-swelling of membranes performed on isothermal TGA scanning, under forced convection conditions (nitrogen flow), showed that the mechanism is accelerated by the presence of MWCNTs (Fig. 2b). In fact, the rate of de-swelling (R) of PVA membranes is $-3\% \text{ min}^{-1}$, which increased about twice in PVA-MWCNTs membranes. De-swelling time (t_{ds}) was taken at constant weight loss that was ca. 8 °C higher than that recorded where volatilization rate change. PVA membrane de-swelled at 37 °C after 42 min (Table 2) under the experimental conditions for TGA recording. This process shifted to lower t_{ds} values on membranes containing MWCNTs, which were about 25 min lower than that of PVA. Furthermore, t_{ds} values did not show relevant difference with composition. On the other hand, the swelling behaviour was distinct in relation to that of de-swelling. Both swelling and de-swelling mechanisms depend on the polymer–solvent interaction. However, in the de-swelling mechanism there is another variable that is the diffusion process. In this case the morphology of membrane is determinant because it defines

the pathway of water transport. So, it is possible that the ionic surfactant present in the MWCNTs aqueous dispersion interacts with the hydroxyl groups of PVA. This can reduce the number of their interactions with water molecules and consequently its SWD. On the other hand, it can also be supposed that in the de-swelling mechanism the presence of the MWCNTs that can hinder somehow water diffusion from the bulk of membrane is compensated by the fewer amounts of interacted water molecules, which facilitate its volatilization. Another hypothesis can be associated to the time and/or way of removing excess of surface water from membrane.

SWD value of sample PVNT1 was of 308% that is about 14% higher than that of PVA membrane. However, the value of SWD decreased with increasing of the MWCNTs concentration in the membrane and was 174% for PVNT3 that is about 64% lower than that of PVA.

The effect of MWCNTs on PVA based membranes can be observed in the DSC cooling and second heating traces (Fig. 3). In the present study, the amount range used of MWCNTs to prepare hybrid membranes with PVA was not sufficient to change the amorphous phase as indicated by temperatures of PVA and its membranes around of 76 °C. On the other hand, MWCNTs influence the crystalline phase organization as nucleant of PVA as shown by the difference between PVA and PVNT3 cooling peak temperatures at 196 and 205 °C, respectively.

Figure 3b shows DSC normalized traces recorded at second heating with indication of the onset (T_o) and peak melting (T_m) temperatures. In the present study, the recorded T_m temperatures are analysed as a function of MWCNTs considering that is the temperature of melt of the higher fraction of crystals. T_m value of PVA is 223 °C and slight changes were observed in the PVA-MWCNTs membranes; PVNT2 decreased only of 2 °C whereas PVNT3 increased of 3 °C.

In the initial swelling process of the polymeric membrane the water molecules disrupt its intermolecular hydrogen bonds and then bind to the hydrophilic sites. These water molecules have restricted mobility and capacity to

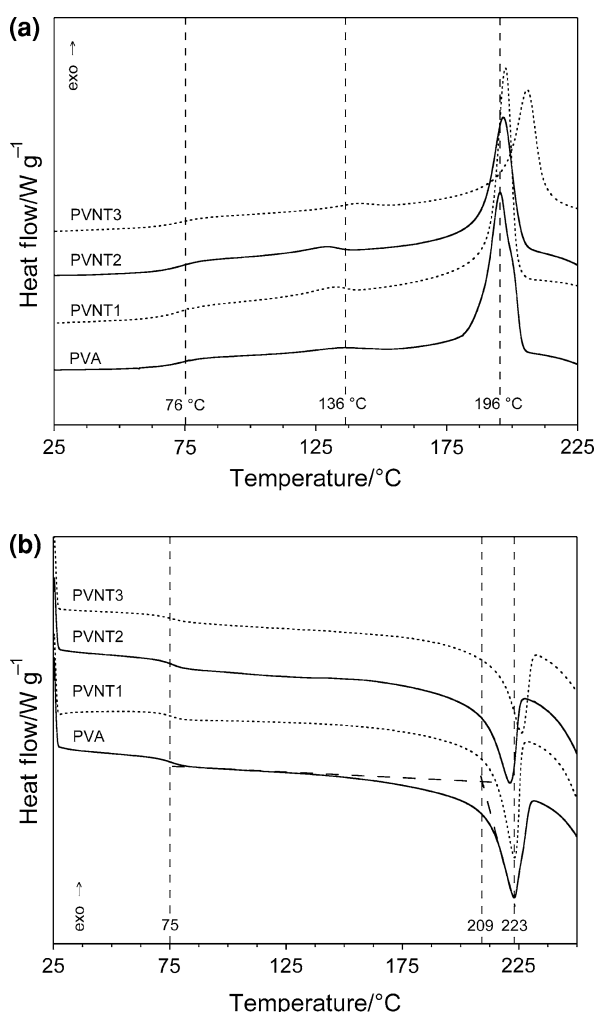


Fig. 3 DSC cooling (a) and second heating (b) traces of PVA and PVA/MWCNTs nanocomposite membranes

crystallize and will be classified “bound water”; another situation that inhibits water mobility inside a membrane is the presence of capillary-like pores. On the other hand, water molecules inside larger pores is free to crystallize and will be classified as “non-bound water” [12, 13]. The amount of *non-bound water* and *bound water* (Fig. 4) was calculated considering that the water molecules into the membranes have equivalent characteristics of pristine water used to swell them [12]. The equations used to calculate these states of water into PVA membrane are the following:

$$w_{nb} = Q_w / \Delta H_w \tag{2}$$

$$w_b = w_t - w_{nb} \tag{3}$$

where, w_{nb} , w_b , and w_t are weight of *non-bound*, *bound* and *total water* into swollen membrane, respectively, and Q_w is the measured heat of crystallization in Joules and ΔH_w is the enthalpy of the ice-water transition obtained from pristine water, whose value measured on DSC trace from cooling scan is 393 J g^{-1} .

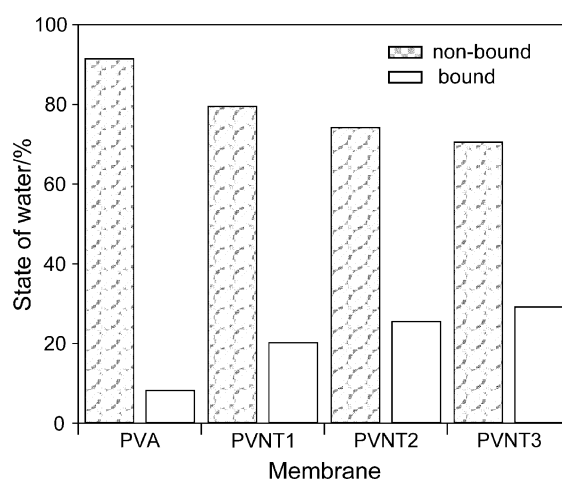


Fig. 4 States of water amount inside PVA and PVA-MWCNTs membranes

The amount of *bound water* increases with increasing of MWCNTs amount in the PVA membranes. As the polymer–water interactions decreased with the increasing of MWCNTs one can correlate this behaviour is correlated with the capillary effect promoted by the interfaces of the MWCNTs with PVA, which prevents the ice formation. Besides, this effect competes with that of PVA hydrophilicity.

Conclusions

Hybrid membranes based on PVA loaded with MWCNTs were prepared and characterized morphologically using SEM and the thermal analysis gave information about PVA thermal stability and de-swelling (TGA) and phase transition and state of water inside of hybrid membranes (DSC). SEM observations showed the presence of MWCNTs agglomerates characterized by a 200–300 nm size. These agglomerates would be one of the factors influencing the amount of non-bound and bound water into the hybrid membranes. The moisture of PVA hybrid membranes in equilibrium with that of ambient increased with increasing of MWCNTs amount going from 7 to 16 wt%. Thermal degradation properties were relevant for compositions containing $50 \times 10^{-2} \text{ w v}^{-1}\%$ of MWCNTs that resulted to be $10 \text{ }^\circ\text{C}$ more stable than PVA. The behaviour of swelling and de-swelling data suggested that the ionic surfactant used to disperse MWCNTs in water has an important role in the hybrid membranes as explained by some apparent contradictory results. The higher amount of MWCNTs presented a nucleant effect as demonstrated by the increasing of $9 \text{ }^\circ\text{C}$ in the crystallization temperature.

Acknowledgements The authors would like to express sincere thanks to “NOE-Expertissues” CT-2004-500328 and PRIN-2006 for supporting the present ongoing research activity at BIOLab of the University of Pisa. Nanocyl SA, Belgium is acknowledged for the kind supply of CNT sample within the framework of the IP-Ambio (NMP4CT2005011827).

References

1. Son SJ, Bai X, Lee SB. Inorganic hollow nanoparticles and nanotubes in nanomedicine. Part 1. Drug/gene delivery applications. *Drug Discov Today*. 2007;12:650–6.
2. Cadek M, Coleman JN, Ryan KP, Nicolosi V, Bister G, Fonseca A, et al. Reinforcement of polymers with carbon nanotubes: the role of nanotube surface area. *Nano Lett*. 2004;4:353–6.
3. Calvert P. Nanotube composites—a recipe for strength. *Nature*. 1999;399:210–1.
4. Lee KY, Mooney DJ. Hydrogels for tissue engineering. *Chem Rev*. 2001;101:1869–79.
5. Tong X, Zheng JG, Lu YC, Zhang ZF, Cheng HM. Swelling and mechanical behaviors of carbon nanotube/poly (vinyl alcohol) hybrid hydrogels. *Mater Lett*. 2007;61:1704–6.
6. Cadek M, Coleman JN, Barron V, Hedicke K, Blau WJ. Morphological and mechanical properties of carbon-nanotube-reinforced semicrystalline and amorphous polymer composites. *Appl Phys Lett*. 2002;81:5123–5.
7. Dureja H, Tiwary AK, Gupta S. Simulation of skin permeability in chitosan membranes. *Int J Pharm*. 2001;213:193–8.
8. Samal SK, Chiellini F, Bartoli C, Fernandes EG, Chiellini E. Hybrid hydrogels based on poly(vinyl alcohol)-chitosan blends and relevant CNT composites. In: Barbucci R, editor. *Hydrogels: biological properties and applications*. Milan: Springer; 2009. p. 67–78.
9. Tanaike O, Kitada N, Yoshimura H, Hatori H, Kojima K, Tachibana M. Lithium insertion behavior of carbon nanowalls by dc plasma CVD and its heat-treatment effect. *Solid State Ionics*. 2009;180:381–5.
10. Fernandes EG, Lombardi A, Solaro R, Chiellini E. Thermal characterization of three-component blends for hot-melt adhesives. *J Appl Polym Sci*. 2001;80:2889–901.
11. Moniruzzaman M, Winey KI. Polymer nanocomposites containing carbon nanotubes. *Macromolecules*. 2006;39:5194–205.
12. Fernandes EG, Krauser S, Samour CM, Chiellini E. Symmetric block oligomers—gelation characteristics by DSC. *J Therm Anal Calorim*. 2000;61:551–64.
13. Chiellini EE, Giannasi D, Solaro R, Chiellini E, Fernandes EG. Hybrid polymeric hydrogels for the controlled release of protein drugs: DSC investigation of water structure. In: Ottenbrite RM, editor. *Frontiers in biomedical polymer applications*. Lancaster: Technomic; 1998. p. 13–25.